THE JOURNAL OF PHYSICAL CHEMISTRY B

Article

pubs.acs.org/JPCB

SANS, Infrared, and ^{7}Li and ^{23}Na NMR Studies on Phase Separation of Alkali Halide−Acetonitrile−Water Mixtures by Cooling

Hiroki Haramaki, Takuya Shimomura,† Tatsuya Umecky, and Toshiyuki Takamuku*

Department of Chemistry and Applied Chemistry, Faculty of Science and Engineering, Saga University, Honjo-machi, Saga 840-8502, Japan

Supporting Information

ABSTRACT: Phase separation of alkali halide (MX) (M = Li^+, Na^+, and K^+ and X = Cl^- and Br^-)−acetonitrile (AN)−water mixtures by cooling has been investigated at the molecular level. The phase diagram obtained for the MX−AN−H_2O ternary systems showed that the temperatures of phase separation for the mixtures with MCl are higher than those with MBr. The phase-separation temperatures of the mixtures with MCl and MBr are higher in the sequence of NaX > KX > LiX, although the magnitude of the hydration enthalpies for the alkali metal ions is larger in the sequence of Li^+ > Na^+ > K^+. To elucidate the reasons for the sequence of phase separation on the meso- and microscopic scales, small-angle neutron scattering (SANS), infrared (IR), and ^{7}Li and ^{23}Na NMR measurements have been conducted on MX−AN−water mixtures with lowering temperature. The results of SANS and IR experiments showed that the mechanism of phase separation of the mixtures by cooling is the same among all of the mixtures but did not clearly reveal the reasons for the phase separation sequence. In contrast, the spin−lattice relaxation rates and the chemical shifts of ^{7}Li and ^{23}Na NMR for the mixtures suggested the different solvation structure of Li^+ and Na^+ in the mixtures. In conclusion, the solvation of acetonitrile molecules for Li^+ and the formation of Li^+−X^- contact ion pairs in the mixtures cause the weakest effect of LiX on phase separation of the mixtures by cooling among the alkali metal ions.

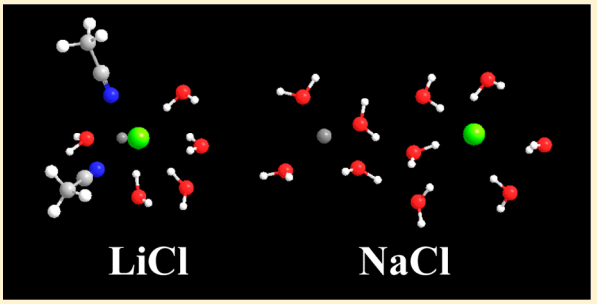

INTRODUCTION

Organic solvents, such as acetonitrile (AN) and 2-butoxyethanol (BE), are miscible with water at any ratio under ambient conditions. However, AN−H_2O mixtures are separated into acetonitrile-rich and water-rich phases as the temperature is lowered. Thus, the mixtures have the upper critical solution temperature (UCST) at 272 K and acetonitrile mole fraction of x_{AN} = 0.38.[1] In contrast, phase separation of BE−H_2O mixtures occurs when the temperature rises: the lower critical solution temperature (LCST) at 323 K and x_{BE} = 0.07.[2] In the previous investigations, the phase equilibria of such water-miscible organic solvent−water mixtures with UCST and LCST have often been discussed on the basis of the thermodynamic parameters.[3−7] The mechanisms for phase separation of such mixtures are understood as follows. In a mixture with UCST, water clusters are gradually evolved by hydrogen bonding among them with lowering temperature; then, organic solvent clusters that are simultaneously formed in the mixtures are excluded from water clusters. Hence, phase separation of the mixtures finally occurs. The weak interactions, such as dipole−dipole interaction, between organic solvent and water molecules are the key to phase separation.[8] In contrast, organic solvent and water molecules form hydrogen bonds between them in a mixture with LCST. However, the hydrogen bonds are disrupted with increasing temperature. Finally, the interactions between water clusters and organic solvent clusters are broken to form two phases.

Many researchers have made efforts to directly observe the process of phase separation of mixtures at the molecular level using various techniques, such as light scattering[2] and small-angle X-ray scattering (SAXS).[9] Small-angle neutron scattering (SANS) is one of the most powerful tools to clearly observe clusters formed in binary mixtures. The difference of the neutron scattering powers of proton H and deuterium D (−3.74 and 6.67 fm, respectively) may highly contrast deuterated solvent molecules with undeuterated ones, such as a combination of CH_3CN and D_2O.

Phase separation of water-miscible organic solvent−water mixtures may also take place without cooling or heating as suitable salt is added into the mixtures. This is called as salting-out and has been discussed in terms of parameters of electrostatics,[10] thermodynamics,[11−14] and statistical-mechanics[15−17] in the early stage. The mechanism of salt-induced phase separation of binary mixtures may also be clarified from the direct observation of the growth of clusters using SANS technique. We have investigated sodium chloride-induced phase separation of AN−D_2O[18,19] and 1,4-dioxane−D_2O

Received: October 6, 2012
Revised: January 21, 2013
Published: January 29, 2013

mixtures[20] by means of SANS. The results showed that water clusters are evolved with increasing salt content. Inherently, the organic solvent molecules and water molecules form the respective clusters in AN−water[18,19] and 1,4-dioxane−water[21] mixtures, and thus both mixing states are heterogeneous on the microscopic scale. The heterogeneity of the mixtures is enhanced on adding salt because water clusters are grown up around Na^+ and Cl^- due to the preferential solvation of water for both ions. This arises from the higher electron donicity (Gutmann's donor number D_N = 18.0) and acceptability (Mayer−Gutmann's acceptor number A_N = 54.8) of water compared with those of the organic solvents (D_N = 14.1 and A_N = 19.3 for acetonitrile and D_N = 14.8 and A_N = 10.8 for 1,4-dioxane).[22] When water clusters exclude organic solvent clusters, phase separation occurs even at an ambient temperature as well as temperature-induced phase separation of binary mixtures. Hence, the mechanism of salt-induced phase separation is also simple.

In the previous investigation, however, we have found the strange sequence of alkali chloride-induced phase separation of AN−water mixtures at 298 K. Thus, phase separation of the mixtures more easily occurs at the lower salt concentration in the sequence of NaCl < KCl < LiCl.[23] This is inconsistent with the magnitude of the hydration enthalpies of the alkali metal ions (−531, −416, and −334 kJ mol^{-1} for Li^+, Na^+, and K^+, respectively).[24] Normally, one can predict that phase separation of AN−water mixtures most easily takes place on adding LiCl among the alkali chlorides because Li^+ strongly attracts the largest amount of water. However, the fact upset the prediction. The mechanism of the salt-induced phase separation above is simple but still incomplete. Liquid−liquid phase equilibria of binary mixtures are a classic subject in the physics. However, unknowns for the phase equilibria of mixtures still remain in the chemistry. In fact, the recent development of various techniques allows researchers to find unique phase equilibria of binary mixtures. Although the LCST (310 K, volume ratio ϕ_{3MP} = 0.30) of 3-methylpyridine (3MP)−D_2O mixtures are well known, the formation of onion droplets in the mixtures on addition of sodium tetraphenylborate ($NaBPh_4$) has been recently found using neutron scattering techniques.[25] The 3MP and D_2O molecules concentrically form alternate multithin layers like an onion, where the hydrophobic BPh_4^- and the hydrophilic Na^+ stabilize the onion structure from the 3MP and D_2O phases, respectively. It is thus worthwhile to revisit phase equilibria of water-miscible organic solvent−water mixtures with salts.

In the present investigation, we aimed at clarifying the reasons for the sequence of phase separation of alkali halide (MX)−AN−water mixtures (M = Li^+, Na^+, and K^+ and X = Cl^- and Br^-) on the microscopic scale. To elucidate the mechanism of phase separation from the enhancement of hydrogen bonding among water molecules, the mixtures with a constant concentration of MX were examined with varying temperature. The phase equilibria of mixtures were first displayed into a phase diagram as a function of mixing ratio of acetonitrile to water and temperature. To observe the evolution of water clusters by hydrogen bonding among water, SANS and infrared (IR) experiments were conducted on the mixtures as a function of temperature. Observation of the solvation structure of Li^+ in AN−water mixtures using large-angle neutron scattering (LANS) technique would be a shortcut to our goal. However, the concentration range of MX for phase separation is too low to strictly observe the solvation structure of Li^+ by means of LANS. Thus, we performed ^7Li and ^{23}Na NMR measurements for both relaxation rates and chemical shifts on the mixtures to clarify the solvation structure of Li^+ and Na^+.

EXPERIMENTAL SECTION

Reagents. Acetonitrile (Wako Pure Chemicals, grade for high-performance liquid chromatography) was used without further purification. Doubly distilled water was utilized for preparation of MX−AN−H_2O mixtures, whereas deuterium oxide, D_2O (Cambridge Isotope Laboratories, D atom content of 99.9%), without further purification was employed for preparation of MCl−AN−D_2O mixtures. Lithium chloride, sodium chloride, potassium chloride, lithium bromide, sodium bromide, and potassium bromide (Wako Pure Chemicals, extra grade) were dried at 393 K in an electric oven for 6 h before use. Lithium perchlorate (Wako Pure Chemicals, 98%) was used without further purification. Sodium perchlorate monohydrate (Wako Pure Chemicals, extra grade) was dried over P_2O_5 in a vacuum desiccator.

Phase Diagram. AN−H_2O mixtures at various mole fractions of acetonitrile x_{AN} were first prepared as solvents. Dried salt was then dissolved into the AN−H_2O mixtures at salt concentration of [MX] = 0.10 mol dm^{-3} (hereinafter, the molarity mol dm^{-3} is abbreviated to M). Each sample mixture in a glass vial with a screw stopper was allowed to stand for 24 h in a temperature-controlled water bath at given temperatures within a deviation of ±0.1 K. The sample mixtures gave the results of homogeneous and phase-separated mixtures. The results are indicated as a phase diagram in Figure 1. For SANS experiments, the phase-separation temperatures of MCl−AN−D_2O mixtures were also determined in the same way as above and summarized in Table 1.

SANS Experiments. MCl−AN−D_2O mixtures at x_{AN} = 0.38 and [MCl] = 0.10 M were prepared in a nitrogen-filled glovebox to avoid replacement of D atoms of D_2O by H atoms. According to the phase diagram obtained, SANS measurements were made on the MCl−AN−D_2O mixtures with lowering temperature from 308 K toward each phase-separation

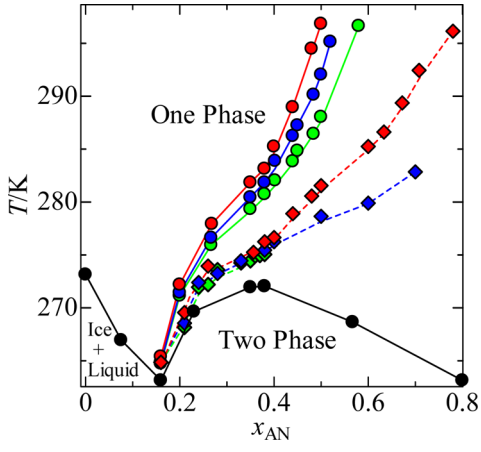

Figure 1. Phase diagram of MX−AN−H_2O (M = Li^+, Na^+, and K^+, X = Cl^- and Br^-) with [MX] = 0.10 M and AN−H_2O mixtures.[1] Circles and diamonds give phase-separation temperatures of the chloride and bromide systems, respectively. The green, red, and blue symbols represent the temperatures of the Li^+, Na^+, and K^+ systems, respectively. The black circles show phase-separation temperatures of the AN−H_2O system.[1] The lines are depicted for the clarity of change in the phase-separation temperatures.

dx.doi.org/10.1021/jp309881v | J. Phys. Chem. B 2013, 117, 2438−2448

Table 1. Phase Separation Temperatures of MCl−AN−D_2O Mixtures at Various Acetonitrile Mole Fractions x_{AN}

sample	x_{AN}	phase separation temperature/K		
		Li^+	Na^+	K^+
MCl−AN−D_2O	0.26	282.7	283.4	283.1
	0.35	286.3	287.9	287.0
	0.38	287.7	290.1	288.2
	0.40	287.9	291.3	289.3
	0.44	289.5	294.6	290.1

temperature. SANS-U spectrometer installed at the reactor JRR-3 in Japan Atomic Energy Agency (JAEA), Tokai, Japan, was used in the present SANS experiments. The sample mixtures were kept into a quartz cell of 10 mm in width, 40 mm in height, and 2 mm in sample thickness. The distances between the sample position and the detector were set at 1 and 4 m, where the momentum transfer q ($= 4\pi\lambda^{-1} \sin\theta$) ranges of 0.04 to 0.35 and 0.015 to 0.075 $Å^{-1}$ were covered, respectively.[26,27] The sample mixtures at the detector positions of 1 and 4 m were exposed to neutron beams (wavelength of λ = 7 Å) for 5 and 30 min, respectively. The size of neutron beams was 5 mm in diameter at the sample position. The deviation of sample temperature was controlled within ±0.1 K during the measurements by circulation of temperature-controlled water in a cell jacket. The transmission by a sample and a cell was measured with a ^3He detector placed at a beam stopper position. The observed intensities were corrected for background by subtraction of intensities of an empty cell and then normalized by dividing the intensities for each sample mixture by those for a standard polyethylene sample, F200-0.[26,27] Densities of the sample mixtures in the temperature range examined were measured using an electronic densimeter (ANTON Paar K. G., DSA5000) for analysis of SANS data. The compositions and densities of all sample mixtures are outlined in Table 2.

IR Measurements. IR spectra for the MCl−AN−H_2O mixtures at x_{AN} = 0.38 with [MCl] = 0.10 M were recorded on a Fourier transform IR spectrometer (JASCO, FT/IR-6100) with lowering temperature. The sample mixtures were kept in a cell with CaF_2 windows separated with a Teflon spacer of 0.5 mm thickness. The light path of the IR spectrometer was purged by dry nitrogen to avoid absorption of moisture and carbon dioxide. The overtones of the O−H stretching vibrations of H_2O in the sample mixtures were observed in the wavenumber range of 6000−7800 cm^{-1}. The spectra were accumulated for 64 times with a resolution of 1 cm^{-1}. The sample temperature was controlled within ±0.1 K during the measurements by circulation of temperature-controlled water in a cell jacket.

^{7}Li and ^{23}Na NMR Spin−Lattice Relaxation Rates. ^7Li NMR spin−lattice relaxation in the LiX−AN−H_2O mixtures may occur through the two mechanisms, quadrupole relaxation of ^7Li and dipole−dipole relaxation between water ^1H atoms and ^7Li.[28] To eliminate the contribution of the dipole−dipole relaxation, ^7Li NMR relaxation measurements at 298 K were made on the LiCl−AN−D_2O mixtures with [LiCl] = 0.020 M over the entire x_{AN} range and the LiBr− and $LiClO_4$−AN−D_2O mixtures with [LiX] = 0.020 and 0.10 M. ^{23}Na NMR spin−lattice relaxation is attributed only to ^{23}Na quadrupole.[29] Thus, ^{23}Na NMR spin−lattice relaxation measurements at 298 K were made on NaCl−, NaBr−, and $NaClO_4$−AN−H_2O mixtures with [NaX] = 0.10 M at various x_{AN}. ^{23}Na NMR measurements were also conducted on NaCl−AN−H_2O mixtures with [NaCl] = 0.020 M for comparison with the ^7Li NMR data at the same concentration. An inversion recovery method was adopted to determine the relaxation times for both LiX and NaX systems. Before measurements, the sample mixtures were degassed by at least five pump−freeze−thaw cycles. All sample mixtures were kept in a 5 mm sample tube (Shigemi, PS-001-7). An FT-NMR spectrometer (Agilent Technologies, 400 MHz NMR system) was used for the ^7Li and ^{23}Na NMR spin−lattice relaxation measurements. During the NMR measurements, the sample temperature was controlled at 298.2 ± 0.1 K by a heater and a dry nitrogen stream generated from liquid nitrogen.

Table 2. SANS Results of Ornstein−Zernike Correlation Lengths ξ (Å) and Scattering Intensities I_0 (cm^{-1}) at q = 0 of MCl−AN−D_2O Mixtures at x_{AN} = 0.38 as a Function of Temperature T (K) together with Densities d (g cm^{-3}) of the Mixtures[a]

sample	x_{AN}	T	ξ	I_0	d
LiCl−AN−D_2O	0.38	288	62.2(3)	24.2(7)	0.92333
		289	49.1(3)	16.8(9)	0.92286
		290	38.7(8)	10.5(8)	0.92201
		291	32.6(8)	7.61(5)	0.92115
		293	26.6(9)	4.68(7)	0.91906
		298	18.4(1)	2.40(1)	0.91460
		303	14.6(5)	1.54(5)	0.91002
NaCl−AN−D_2O	0.38	291	68.1(4)	30.5(6)	0.92843
		293	37.0(2)	9.45(1)	0.92656
		298	21.0(2)	3.29(1)	0.92216
		303	16.3(9)	1.99(2)	0.91763
		308	13.3(1)	1.34(3)	0.91298
KCl−AN−D_2O	0.38	289	76.4(9)	38.9(7)	0.92580
		290	50.3(6)	17.1(9)	0.92496
		291	39.6(4)	10.8(2)	0.92410
		293	30.1(1)	5.75(2)	0.92200
		298	19.2(7)	2.63(2)	0.91754
		303	15.3(6)	1.65(2)	0.91295

[a]Values in the parentheses are estimated standard deviations σ for the last Figure.

^{7}Li and ^{23}Na NMR Chemical Shifts. LiCl−AN−H_2O mixtures with LiCl concentrations of 0.10 and 0.020 M are prepared below and above x_{AN} = 0.6, respectively, because of the limitation of the LiCl solubilities. ^7Li NMR spectra of the LiCl systems at 298.2 ± 0.1 K were recorded on the same spectrometer above. For comparison, the spectra of LiBr−AN−H_2O and $LiClO_4$−AN−H_2O mixtures with [LiX] = 0.10 M over the entire x_{AN} range were also measured at 298.2 ± 0.1 K. ^{23}Na NMR measurements at 298.2 ± 0.1 K were made on NaCl−AN−H_2O mixtures with [NaCl] = 0.020 and 0.10 M and NaBr− and $NaClO_4$−AN−H_2O mixtures with [NaX] = 0.10 M as a function of x_{AN}. Methanol solutions of 3.0 M LiCl and 0.7 M $NaBPh_4$ were sealed into external double reference tubes (Shigemi) as reference substances for ^7Li and ^{23}Na nuclei, respectively. The external double-reference tube, whose dimension is a capillary of 1.5 mm outer diameter with a blown-out sphere of 3 mm at the base, was placed at the center of the 5 mm sample tube containing a sample mixture. The observed chemical shifts of the sample mixtures were corrected for their volume magnetic susceptibilities by an external double-reference method according to the literature.[30−32] The digital

dx.doi.org/10.1021/jp309881v | J. Phys. Chem. B 2013, 117, 2438−2448

resolutions of the chemical shifts for ^{7}Li and ^{23}Na NMR measurements were ±0.0062 and ±0.048 ppm, respectively.

RESULTS AND DISCUSSION

Phase Diagrams. Figure 1 shows the phase-separation temperatures for the MX−AN−H_2O ternary systems as a phase diagram, together with those for AN−H_2O binary system.[1] The solid and dashed lines are drawn for the clarity of the change in the phase-separation temperatures for each system. The mixtures are separated into acetonitrile-rich (upper) and water-rich (lower) phases when the temperature is lowered to the phase-separation temperature. The line of the AN−H_2O system appears as a convex above x_{AN} = 0.16; the UCST for the system is found at 272 K at x_{AN} = 0.38.[1] Below x_{AN} = 0.16, ice is precipitated from AN−H_2O mixtures. The phase-separation temperatures of the MX−AN−H_2O ternary systems above x_{AN} = 0.16 are higher compared with those of the AN−H_2O binary system. The temperatures for the ternary systems increase with increasing x_{AN}. As discussed in the previous reports,[18,19] water clusters are easily evolved around cations and anions in the mixtures even at the higher temperatures due to the preferential solvation of both ions by water molecules. The electron donicity and acceptability of water are much higher compared with those of acetonitrile, respectively.[22]

The phase-separation temperatures of the MX−AN−H_2O ternary systems significantly increase above $x_{AN} \approx 0.38$, resulting in a break point at the mole fraction. This may be related to the UCST of the binary system. In our previous SANS investigation on AN−water mixtures with lowering temperature, the heterogeneity of the mixtures most enhances around the mole fraction of UCST ($x_{AN} \approx 0.38$) as the temperature decreases.[33] Thus, water clusters and acetonitrile clusters are equally formed in the mixture at $x_{AN} \approx 0.38$. Probably, the smaller amount of water clusters in the mixtures above $x_{AN} \approx 0.38$ is more easily eliminated from acetonitrile clusters on adding alkali halide compared with the mixtures below the mole fraction. This is the plausible reason for the break point and the significant increase in the phase separation temperatures above $x_{AN} \approx 0.38$.

The phase-separation temperatures of the MCl systems are higher than those of the MBr systems. Hence, the MCl systems are more easily separated at the higher temperatures compared with the MBr systems. This can be readily expected from the magnitude of the hydration enthalpies for Cl^- and Br^- (−367 and −336 kJ mol^{-1}) at 298 K.[24] Water clusters are more easily evolved around Cl^- in the chloride systems at the higher temperatures compared with the bromide systems. The cation dependence of the phase-separation temperatures of both MCl and MBr systems in the range of x_{AN} > 0.16 is of interest. The phase-separation temperatures for each MX system are higher in the sequence of $Na^+ > K^+ > Li^+$. This does not agree with the magnitude of the hydration of the alkali metal ions (the hydration enthalpies of −531, −416, and −334 kJ mol^{-1} for Li^+, Na^+, and K^+, respectively).[24] As seen in Table 1, the phase-separation temperatures for the MCl−AN−D_2O systems are also higher in the same sequence. The present results on the MCl−AN−water systems with lowering temperature are the same as the previous results on the systems at the constant temperature of 298 K with increasing MCl concentration.[18,19] Thus, other factors, except for the magnitude of hydration of the alkali metal ions, should contribute to the sequence of phase separation of the MCl− and MBr−AN−water mixtures by cooling.

SANS Experiments. Figure 2 shows the normalized SANS intensities for LiCl−, NaCl−, and KCl−AN−D_2O mixtures at

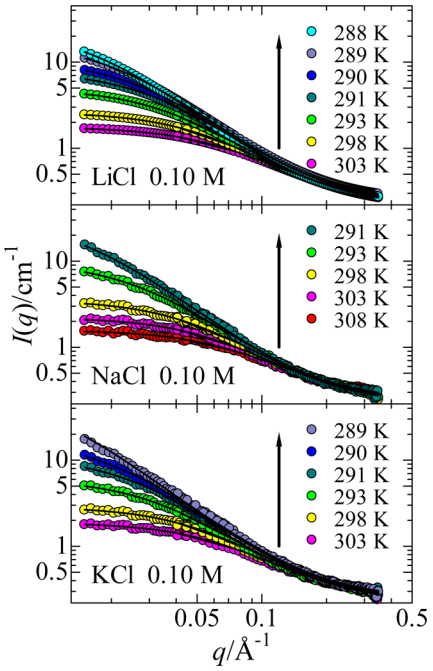

Figure 2. SANS intensities of MCl−AN−D_2O mixtures at x_{AN} = 0.38 and [MCl] = 0.10 M as a function of temperature. The circles give the observed intensities of the mixtures. The solid lines indicate the results of least-squares fits using eq 1. The arrows indicate the lowering of the temperature.

x_{AN} = 0.38 and various temperatures below each phase-separation temperature as a function of q. The SANS intensities for each system are gradually strengthened with decreasing temperature toward the phase separation temperature. This suggests that D_2O clusters and acetonitrile clusters are gradually evolved in the mixtures when the temperature decreases because the SANS measurements observed the contrast between D_2O as a strong neutron scatterer and acetonitrile as a weak one. Ornstein−Zernike fits were performed on the SANS intensities of the mixtures using a least-squares refinement procedure through

$$I(q) = \frac{I_0}{1 + \xi^2 q^2} + \text{B.G.} \quad (1)$$

Here I_0 and ξ give the SANS intensity at q = 0 and the correlation length, respectively, and B.G. is background. The correlation length ξ is the decay factor of the exponential decrease in the number of clusters with increasing their size;[9,34] the larger the ξ value, the larger the clusters in a solution. In Table 2, I_0 and ξ determined for the MCl−AN−D_2O mixtures at each temperature are summarized. Figure 3 shows that the ξ values become larger in the sequence of $Na^+ > K^+ > Li^+$ as the temperature decreases. This agrees with the sequence of the phase-separation temperatures for the $Na^+ > K^+ > Li^+$ systems. Thus, D_2O clusters are more easily evolved in the mixtures at the higher temperature in the same sequence.

To clarify the mechanism of evolution of water clusters with lowering temperature, critical exponents were determined from the temperature dependence of I_0 and ξ. In Figure 4, the logarithmic I_0 and ξ of the mixtures at x_{AN} = 0.38 are plotted

dx.doi.org/10.1021/jp309881v | J. Phys. Chem. B 2013, 117, 2438−2448

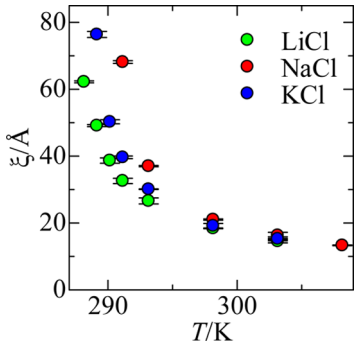

Figure 3. Ornstein–Zernike correlation lengths ξ of MCl–AN–D_2O mixtures at x_{AN} = 0.38 and [MCl] = 0.10 M as a function of temperature. The standard deviations σ are indicated by error bars.

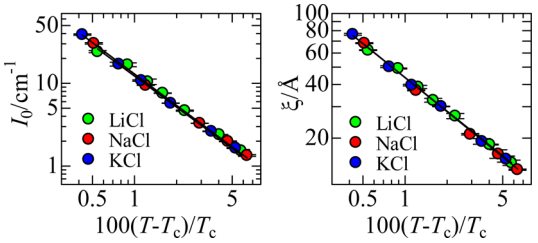

Figure 4. I_0 and ξ values (circles) of MCl–AN–D_2O mixtures at x_{AN} = 0.38 and [MCl] = 0.10 M as a function of normalized temperature. The solid lines are the results of least-squares fits on the values using eqs 2 and 3, respectively. The standard deviations σ are indicated by error bars.

against the logarithmic normalized temperature, $(T-T_c)/T_c$, where T_c is the phase-separation temperature (Table 1). The I_0 and ξ values near T_c can be expressed by

$$I_0 = I_{bare}\left[\frac{T_c - T}{T_c}\right]^{-\gamma} \quad (2)$$

$$\xi = \xi_{bare}\left[\frac{T_c - T}{T_c}\right]^{-\nu} \quad (3)$$

where I_{bare} and ξ_{bare} are the bare I_0 and ξ, respectively, and γ and ν are critical exponents.[35] In the logarithmic plots of Figure 4, the slopes of the plots correspond to the critical exponents of γ and ν, whereas the intercepts are the I_{bare} and ξ_{bare}. A least-squares refinement procedure through eqs 2 and 3 was made on the experimental values. The γ and ν values estimated are summarized in Table 3. All of the critical exponents for the three systems are very close to the typical values for the 3D-Ising mechanism of γ = 1.24 and ν = 0.63.[35] Actually, the plots for the three MCl–AN–D_2O systems almost overlap among them. The critical exponents show that phase separation of the MCl–AN–D_2O mixtures by cooling occurs through the 3D-Ising mechanism. Thus, the mechanism for the evolution of D_2O clusters with lowering temperature does not depend on the alkali metal ions. However, the SANS experiments do not clarify the reason why LiCl less easily induces evolution of water clusters in the mixtures despite the strongest hydration for Li^+ among the alkali metal ions.

Table 3. Critical Exponents γ and ν for MCl–AN–D_2O Mixtures at x_{AN} = 0.38

sample	x_{AN}	γ	ν
LiCl–AN–D_2O	0.38	1.25	0.63
NaCl–AN–D_2O	0.38	1.26	0.64
KCl–AN–D_2O	0.38	1.27	0.63

IR Measurements. Figure 5 shows IR spectra for the MCl–AN–H_2O mixtures at x_{AN} = 0.38 and [MCl] = 0.10 M in the wavenumber range of 6000–7800 cm^{-1} as a function of temperature. For all of the systems, the intensity of a peak at ~7000 cm^{-1} decreases with cooling, whereas that at ~6800 cm^{-1} increases. These peaks are assigned to the overtones of the O–H stretching vibrations of H_2O molecules, suggesting that two states of water molecules exist at least in the mixtures. The spectra in the range of 6000–7800 cm^{-1} were deconvoluted through pseudo-Voigt functions. The representative result of the deconvolution is depicted in Figure 6. Small peaks of the C–H stretching vibrations of acetonitrile molecule are observed at 7200, 6852, 6557, and 6277 cm^{-1}. Four

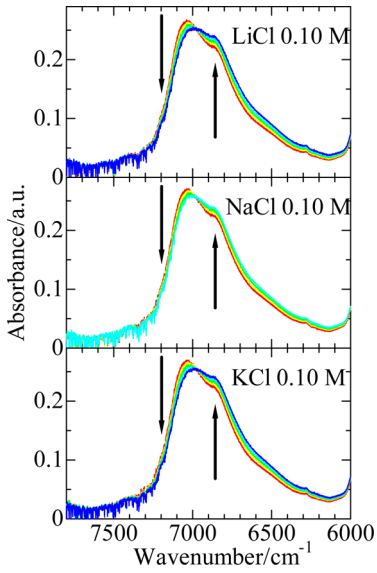

Figure 5. IR spectra of MCl–AN–H_2O mixtures at x_{AN} = 0.38 and [MCl] = 0.10 M in the wavenumber range of 6000–7800 cm^{-1} as a function of temperature. The arrows indicate the lowering of temperature.

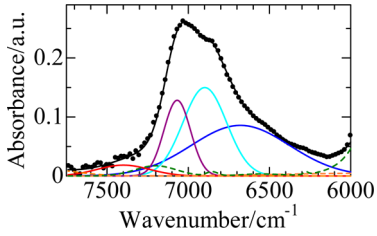

Figure 6. Representative results of deconvolution for IR spectra of NaCl–AN–H_2O mixture at x_{AN} = 0.38 and [MCl] = 0.10 M through pseudo-Voigt functions. The dots and the black solid line give the experimental values and the total theoretical ones, respectively. The blue and pale-blue lines represent the overtone components of the symmetry and asymmetry O–H stretching vibrations of hydrogen-bonded water, respectively. The purple and red lines give those of isolated water, respectively. The green dashed line indicates the overtone components of the C–H stretching vibrations of acetonitrile, and the orange line displays background.

dx.doi.org/10.1021/jp309881v | J. Phys. Chem. B 2013, 117, 2438–2448

overtones of the O−H vibrations can be extracted by the deconvolution. Two broad peaks at 6689 and 6903 cm^{-1} are assigned to the overtones of the symmetric and asymmetric O−H vibrations of hydrogen-bonded water molecules, respectively.[36] The peaks at 7073 and 7389 cm^{-1} are attributed to the overtones of the symmetric and asymmetric O−H vibrations of isolated water molecules.[36] As seen, the total values of the components well explain the observed values.

To evaluate the formation of the hydrogen bonds among water molecules with lowering temperature, the peak areas of the symmetric O−H vibration components of hydrogen-bonded and isolated water molecules are plotted as a function of temperature in Figure 7. The area of the former linearly

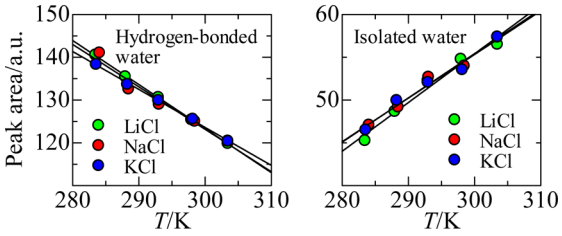

Figure 7. Peak areas (circles) for the overtones of the symmetric O−H vibrations of hydrogen-bonded and isolated water molecules in MCl−AN−H_2O mixtures at x_{AN} = 0.38 and [MCl] = 0.10 M as a function of temperature. The solid lines are the results of least-squares fits on the areas using a linear function.

increases with decreasing temperature, whereas that of the latter decreases. Thus, water molecules gradually enhance water clusters by hydrogen bonding among themselves in all of the mixtures as the temperature is lowered. The slopes of the areas of both vibrations against temperature were estimated by least-squares fits through a linear function. The slopes estimated are summarized in Table 4. The values of the mixtures are not

Table 4. Slopes for the Plots of the Peak Areas for the Overtones of the Symmetric O−H Vibrations of Hydrogen-Bonded and Isolated Water Molecules in MCl−AN−H_2O Mixtures at x_{AN} = 0.38

sample	x_{AN}	hydrogen-bonded water	isolated water
LiCl−AN−H_2O	0.38	−1.03	0.570
NaCl−AN−H_2O	0.38	−0.991	0.517
KCl−AN−H_2O	0.38	−0.991	0.510

significantly different among them. This suggests that the hydrogen bonds among water molecules are evolved in a similar way among all of the MCl systems. Consequently, the IR experiments show that the evolution of water clusters by hydrogen bonding is the key to phase separation of the mixtures by cooling. However, the reason for the sequence (NaCl > KCl > LiCl) of phase separation of the MCl−AN−H_2O mixtures is still not made clear by the IR experiments.

^{7}Li and ^{23}Na NMR Spin−Lattice Relaxation Rates. The SANS and IR measurements cannot elucidate the reason for the weakest effect of Li^+ on phase separation of the MCl−AN−water mixtures among the alkali metal ions. This may be because both SANS and IR techniques mainly give us information on the bulk water in the ternary systems due to its higher concentration but not on the hydration water molecules for the alkali metal ions as cores of water clusters. Hence, we conducted ^{7}Li and ^{23}Na NMR spin−lattice relaxation measurements at 298 K on the MCl−AN−water mixtures (M = Li^+ and Na^+) to clarify the solvation structure of the alkali metal ions from the motion of cations. In addition, the spin−lattice relaxation measurements were made on the bromide and perchlorate (MBr and $MClO_4$) systems to elucidate effects of the anions on the solvation structure of the alkali metal ions. However, the relaxation measurements could not be performed on the KX systems because of the low-resonance frequency of ^{39}K, which cannot be observed with our spectrometer. The ^{7}Li and ^{23}Na spin−lattice relaxation rates determined for the MX−AN−water mixtures at 298 K are summarized in Table S1 in the Supporting Information.

The left panel of Figure 8 shows the relaxation rates of ^{7}Li for the LiCl−, LiBr−, and $LiClO_4$−AN−D_2O mixtures with [LiX] = 0.020 M at 298 K as a function of x_{AN}. The rates of the Li^+ systems gradually increase with increasing x_{AN} to 0.9, showing that the motion of Li^+ is restricted with increasing acetonitrile content. This is because the hydration shell of Li^+ becomes more rigid due to the enhancement of hydrophobic atmosphere around the hydrated Li^+ with the increase in the x_{AN}. The relaxation rates of all the Li^+ systems overlap among them below x_{AN} = 0.8. However, the anion effect on the relaxation rates is significant in pure acetonitrile (x_{AN} = 1). The relaxation rates of the LiBr and $LiClO_4$ systems conspicuously decrease at x_{AN} = 1, revealing that the motion of Li^+ is faster. This is attributed to the weaker solvation of acetonitrile molecules for Li^+ compared with water molecules. In contrast, the relaxation rate of the LiCl system remarkably increases at x_{AN} = 1, showing the strong restriction of the motion of Li^+. This may arise from the formation of Li^+−Cl^- contact ion pair in the acetonitrile solution. As shown in the previous investigation on acetonitrile solution of LiBr by LANS,[37] the four sites of the tetrahedral Li^+ solvation shell are occupied by three acetonitrile

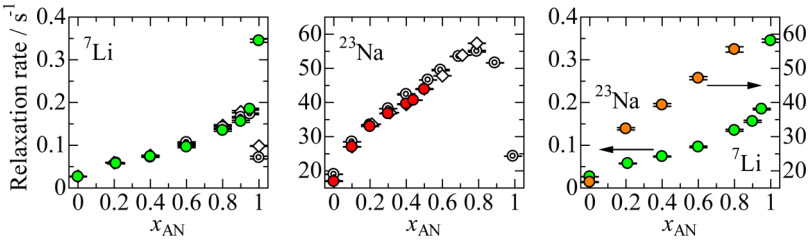

Figure 8. ^{7}Li and ^{23}Na NMR relaxation rates of LiX−AN−D_2O mixtures with [LiX] = 0.020 M and NaX−AN−H_2O mixtures with [NaX] = 0.10 M at 298 K as a function of x_{AN} in the left and central panels, respectively. The green and red circles give the relaxation rates for the LiCl and NaCl systems, respectively. The diamond and double circles represent those of the MBr and $MClO_4$ systems, respectively. In the right panel, the relaxation rates of LiCl−AN−D_2O and NaCl−AN−H_2O (orange circles) mixtures with [MCl] = 0.020 M are plotted against x_{AN} for comparison at the same MCl concentration. The standard deviations σ are indicated by error bars.

dx.doi.org/10.1021/jp309881v | J. Phys. Chem. B 2013, 117, 2438−2448

molecules and one Br^-, and thus the contact ion pairs of Li^+–Br^- form in acetonitrile. The contact of Cl^- with Li^+ in the first solvation shell retards the motion of Li^+ in the LiCl mixtures.

The concentration dependence of the relaxation rates of the LiX–AN–D_2O mixtures was then examined. The relaxation rates of ^{7}Li for the LiBr– and $LiClO_4$–AN–D_2O mixtures with [LiX] = 0.10 M at 298 K were measured and plotted as a function of x_{AN} in Figure 9. For comparison, the rates of the

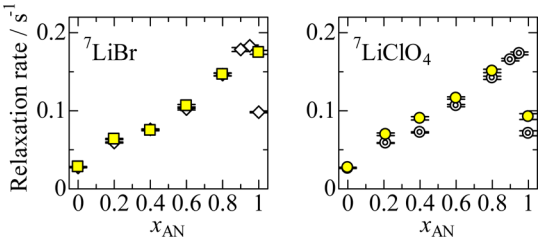

Figure 9. ^{7}Li NMR relaxation rates of LiBr– and $LiClO_4$–AN–D_2O mixtures with [LiX] = 0.10 M at 298 K (yellow squares and circles, respectively) as a function of x_{AN}, together with those at 0.020 M (diamonds and double circles, respectively), which are the same values as those in Figure 8. The standard deviations σ are indicated by error bars.

mixtures with [LiX] = 0.020 M, which are the same as the rates in Figure 8, are also depicted. However, the rates of the LiCl systems with [LiCl] = 0.10 M were not measured because of the limitation of the LiCl solubility. The relaxation rates of the LiBr– and $LiClO_4$–AN–water mixtures at [LiX] = 0.10 M below x_{AN} = 0.8 do not remarkably differ from those at [LiX] = 0.020 M. In acetonitrile (x_{AN} = 1), however, the rate of the LiBr system significantly increases with increasing salt concentration from 0.020 to 0.10 M. The increase in the relaxation rates is ascribed to the formation of Li^+–Br^- contact ion pairs in the acetonitrile solutions at the higher concentration. In contrast, the difference between the relaxation rates of the $LiClO_4$ systems at x_{AN} = 1 with [$LiClO_4$] = 0.020 and 0.10 M is very small. Thus, ClO_4^- scarcely contacts with Li^+ even at the higher concentration. The present ^{7}Li NMR relaxation experiments suggest that Li^+ more easily forms contact ion pairs in the acetonitrile solutions in the sequence of LiCl > LiBr ≫ $LiClO_4$. This finding is reasonable with the basicity of the anions.

The central panel of Figure 8 indicates the relaxation rates of ^{23}Na for the NaCl–, NaBr–, and $NaClO_4$–AN–H_2O mixtures with [NaX] = 0.10 M at 298 K as a function of x_{AN}. The relaxation rates of ^{23}Na NMR of the three systems overlap among them below x_{AN} = 0.5. For the NaCl system above x_{AN} = 0.5, the rates could not be measured because of phase separation of the system. The rates for the NaBr system above x_{AN} = 0.8 could not be determined due to the same. Nevertheless, the increase in the relaxation rates of Na^+ in the NaX–AN–H_2O mixtures with increasing x_{AN} is observed. This suggests that the hydration shell of Na^+ gradually becomes stronger due to the evolution of the hydrophobic atmosphere around the hydrated cations with increasing x_{AN}. It is noteworthy that the increase in the relaxation rates of all the Na^+ system is significant with increasing x_{AN} from 0 to 0.1. This results in a break point at x_{AN} = 0.1. In contrast, a break point is not clearly observed in the relaxation rates of the Li^+ systems below x_{AN} = 0.9. These findings reveal that the hydration shell of Na^+ is significantly strengthened, even on adding a small amount of acetonitrile. The remarkable decrease in the rate of the $NaClO_4$–AN–H_2O mixtures above x_{AN} = 0.9 suggests the weak solvation of acetonitrile molecules for Na^+ as well as Li^+. Probably, acetonitrile molecules might solvate Na^+ in both NaCl– and NaBr–AN–H_2O mixtures at high acetonitrile contents. However, water clusters are evolved enough to separate the NaCl and NaBr systems into two phases before the solvation of acetonitrile for Na^+. This is also the evidence of the easy evolution of water clusters in the NaCl and NaBr systems compared with the LiCl and LiBr systems.

For comparison between the ^{7}Li and ^{23}Na NMR data at the same MCl concentration, the relaxation rates of the LiCl– and NaCl–AN–H_2O mixtures with [MCl] = 0.020 M at 298 K are plotted against x_{AN} in the right panel of Figure 8. The relaxation rates of the NaCl system above x_{AN} = 0.8 still could not be measured because of the solubility of NaCl even at [MCl] = 0.020 M. As seen in the central and right panels of Figure 8 and Table S1 of the Supporting Information, the rates of the NaCl system do not significantly depend on the NaCl concentrations. The increase in the rates of the Na^+ system with increasing x_{AN} from 0 to 0.8 is more significant than that of the Li^+ system. This suggests that the hydration shell of Na^+ is more easily strengthened with the increase in x_{AN} compared with that of Li^+. Hence, water clusters around cations are more easily evolved in the NaCl system than the LiCl one. The results of the NMR relaxation measurements agree with those from the SANS experiments. Despite the absence of the value at x_{AN} = 1, the relaxation rates of the NaCl system seem to be saturated above x_{AN} = 0.8 but might not largely increase above the mole fraction, as seen for the LiCl system. It is suggested thus that

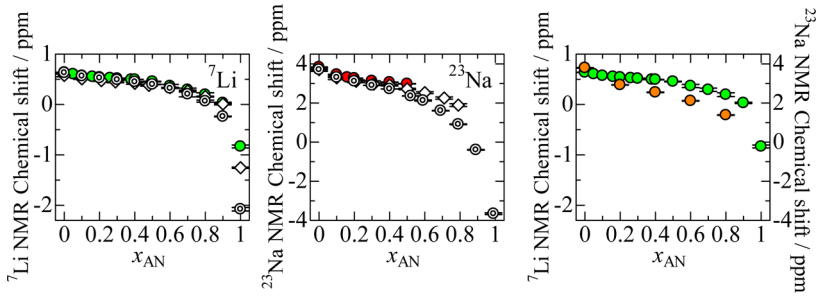

Figure 10. ^{7}Li and ^{23}Na NMR chemical shifts of LiX– and NaX–AN–H_2O mixtures with [MX] = 0.10 M at 298 K as a function of x_{AN} in the left and central panels, respectively, except for the LiCl system above x_{AN} = 0.6 with [LiCl] = 0.020 M. In the right panel, the chemical shifts of NaCl–AN–H_2O mixtures with [NaCl] = 0.020 M for comparison with those of LiCl–AN–H_2O mixtures, which are the same values as those in the left panel. The symbols are the same as those used in Figure 8. The standard deviations σ are indicated by error bars.

dx.doi.org/10.1021/jp309881v | J. Phys. Chem. B 2013, 117, 2438–2448

Na^+-Cl^- contact ion pairs are scarcely formed in the NaCl system.

^{7}Li and ^{23}Na NMR Chemical Shifts. The ^{7}Li and ^{23}Na NMR chemical shifts of the MX−AN−H_2O mixtures were measured at 298 K to elucidate the solvation structure of Li^+ and Na^+ in the mixtures from the change in their electron densities with increasing x_{AN}. Both ^{7}Li and ^{23}Na chemical shifts determined for the mixtures were listed in Table S2 in the Supporting Information. The left panel of Figure 10 shows the chemical shifts of ^{7}Li NMR for the LiCl−AN−H_2O mixtures with [LiCl] = 0.10 and 0.020 M below and above x_{AN} = 0.6, respectively, as a function of x_{AN}. The chemical shifts for the mixtures at both concentrations are smoothly connected at x_{AN} = 0.6. In the same panel, the chemical shifts of the LiBr− and $LiClO_4$−AN−H_2O mixtures with [LiX] = 0.10 M at 298 K are also plotted against x_{AN}. The ^{7}Li chemical shifts of all LiX systems overlap among them below x_{AN} = 0.7. Li^+ ions in the mixtures are moderately shielded as the x_{AN} increases. Above x_{AN} = 0.7, the shielding becomes more significant. Li^+ ions are more remarkably shielded with increasing x_{AN} in the sequence of $LiClO_4$ > LiBr > LiCl. The difference of the chemical shifts among the LiX systems at x_{AN} = 1 is the most significant over the entire x_{AN} range. This feature is comparable with the ^{7}Li NMR relaxation rates of the mixtures. Thus, the change in the ^{7}Li chemical shifts of the mixtures with increasing x_{AN} may be mainly governed by the solvation structure of Li^+ in the mixtures. As discussed on the ^{7}Li NMR relaxation rates, the moderate shielding of Li^+ below x_{AN} = 0.7 suggests the strengthening of the hydration of Li^+ because the hydrophobic atmosphere gradually surrounds the hydrated Li^+ due to the increase in the x_{AN}. This leads to the enhancement of water clusters around Li^+ with lowering temperature, as observed by the SANS measurements. Above x_{AN} = 0.7, the remarkable shielding of Li^+ with increasing x_{AN} is ascribed to the solvation of acetonitrile molecules for Li^+ in the mixtures. Hence, water molecules in the first solvation shell of Li^+ may be gradually replaced by acetonitrile molecules above x_{AN} = 0.7. The cone region of the nitrogen atom of acetonitrile molecule with respect to the C≡N axis is a magnetic shielding field. Thus, Li^+ ions are shielded in the cone when the acetonitrile nitrogen solvates Li^+. Li^+ ions in the AN−H_2O mixtures may be solvated by not only water molecules but also acetonitrile ones, particularly above x_{AN} = 0.7. As discussed on the ^{7}Li NMR relaxation rates, the sequence of the shielding of Li^+ at x_{AN} = 1 arises from the formation of contact ion pairs. Li^+ ions in the LiCl and LiBr systems may form contact ion pairs with the anions, whereas the ion pairs scarcely form in the $LiClO_4$ system due to the much lower charge density of ClO_4^-. Thus, the solvation numbers of acetonitrile for Li^+ in the LiCl and LiBr systems may be smaller compared with that in the $LiClO_4$ system due to the contact of Cl^- and Br^-. As seen in Figure 10, indeed, the shielding of Li^+ in the systems above x_{AN} = 0.7 is weaker in the sequence of LiCl < LiBr < $LiClO_4$. This suggests that Li^+-Cl^- ion pairs most stably form in the system. The ^{7}Li chemical shifts show that contact ion pairs of Li^+-Cl^- form in the mixtures even at x_{AN} = 0.7. Thus, the formation of contact ion pairs of Li^+-X^- in the AN−H_2O mixtures is more sensitively observed by the ^{7}Li chemical shifts measurements compared with the relaxation rate measurements. This is because the former can directly detect the variation in the electron density of Li^+ due to the change in the solvation structure.

The central panel of Figure 10 indicates the ^{23}Na chemical shifts of NaCl−, NaBr−, and $NaClO_4$−AN−H_2O mixtures with [NaCl] = 0.10 at 298 K as a function of x_{AN}. The ^{23}Na NMR data for the NaCl and NaBr systems above x_{AN} = 0.5 and 0.8, respectively, are absent from the Figure because phase separation of the mixtures occurs as described above. Na^+ ions in all NaX systems are gradually shielded against the increase in the x_{AN} as well as the LiX systems. This indicates the strengthening of the hydration for Na^+ due to the hydrophobic atmosphere of acetonitrile. A small step at x_{AN} = 0.1 is found in the change in the Na^+ chemical shifts of the systems with increasing x_{AN}. This is coincident with the ^{23}Na NMR relaxation rates. It is shown again that the hydration shell of Na^+ becomes stronger even on adding a small amount of acetonitrile. The shielding of Na^+ in the $NaClO_4$ system above $x_{AN} \approx 0.3$ is stronger compared with those of the NaCl and NaBr systems, particularly, above $x_{AN} \approx 0.7$. This suggests that water molecules in the first solvation shell of Na^+ in the $NaClO_4$ system may be more easily replaced by acetonitrile molecules, probably due to the hydrophobic atmosphere generated by ClO_4^- compared with the NaCl and NaBr systems. In fact, $MClO_4$ cannot induce phase separation of AN−water mixtures in the present temperature range because water clusters are not easily evolved around ClO_4^- due to the solvation of acetonitrile for ClO_4^-. On the contrary, the hydration for Na^+ in the NaCl and NaBr systems may be more stable.

In the right panel of Figure 10, for comparison, the ^{23}Na NMR chemical shifts of the NaCl−AN−H_2O mixtures with [NaCl] = 0.020 M are depicted as a function of x_{AN}, together with the ^{7}Li NMR chemical shifts of the LiCl−AN−H_2O mixtures, which are the same as those in the left panel. The shielding of Na^+ against the increase in the x_{AN} is more sensitive compared with that of Li^+. This suggests that the hydration for Na^+ is more easily strengthened with increasing x_{AN} than Li^+, as described above. As shown in the central and right panels of Figure 10 and Table S2 in the Supporting Information, the chemical shifts of the NaCl system with [NaCl] = 0.020 M at high x_{AN} are decreased comparably with the values of the $NaClO_4$ system with [$NaClO_4$] = 0.10 M rather than those of the NaCl and NaBr systems with [NaX] = 0.10 M. This implies that Na^+-Cl^- ion pairs are hardly formed in the NaCl system at [NaCl] = 0.020 M. In contrast, Li^+-Cl^- ion pairs are easily formed in the LiCl system even at the same concentration of [LiCl] = 0.020 M, as discussed above.

The ^{7}Li and ^{23}Na NMR results from both relaxation rate and chemical shift measurements clearly show the different solvation structure of Li^+ and Na^+ in the AN−water mixtures. Li^+ ions may be more easily solvated by acetonitrile molecules compared with Na^+ ions. This is attributed to the higher charge density of Li^+; Li^+ ions may attract not only water molecules but also acetonitrile molecules despite the lower electron donicity of acetonitrile than water. Furthermore, both NMR results on the anion effects reveal that Li^+ more strongly contacts with Cl^- to form ion pair in the AN−water mixtures. The ion pairs of Li^+-Br^- may also be formed in the mixtures, whereas those of $Li^+-ClO_4^-$ are hardly formed. The solvation of acetonitrile molecules for Li^+ and the formation of Li^+-X^-contact ion pairs prevent the growth of water clusters in the mixtures as the temperature is lowered. These two factors might not be clarified by LANS because the LiX concentration range for phase separation is too low to observe the solvation structure of Li^+. Both NMR relaxation and chemical shift

dx.doi.org/10.1021/jp309881v | J. Phys. Chem. B 2013, 117, 2438−2448

measurements finally make clear that the two factors are the reasons for the weakest effect of Li^+ on phase separation of the AN−water mixtures by cooling.

Phase Separation Mechanism. The present investigation shows that the phase-separation temperatures of AN−water mixtures rise on adding alkali halides. This is caused by the preferential solvation for the alkali metal ions, chloride, and bromide ions by water molecule due to the higher electron donicity and acceptability of water compared with those of acetonitrile. Thus, the preferential solvation of water molecules for both cations and anions aids the evolution of water clusters by cooling. The anion effect on the increase in the phase-separation temperature is consistent with the magnitude of the hydration enthalpies of Cl^- and Br^-. Hence, water clusters are more easily evolved around Cl^- than Br^-. However, the phase-separation temperatures of the MCl− and MBr−AN−water mixtures are higher in the sequence of the $Na^+ > K^+ > Li^+$ systems, although the magnitude of the hydration enthalpies is larger in the sequence of $Li^+ > Na^+ > K^+$ due to the charge density of the ions that depends on the ionic radius.

The SANS measurements on the MCl−AN−D_2O mixtures reveal that water clusters are gradually evolved in the mixtures as the temperature decreases. Thus, the hydrogen bonds among water molecules increase in the mixtures at the lower temperatures. In fact, the IR measurements on the overtones of the O−H stretching vibrations of water molecules show the increase in the hydrogen bonds among water molecules in the mixtures as the temperature is decreased. When water clusters evolved around both cations and anions exclude acetonitrile clusters, phase separation finally occurs. Although the absolute values of the phase-separation temperatures of the MCl−AN−water mixtures are different among the alkali metal ion systems, the critical exponents of the mixtures estimated from the SANS measurements show that phase separation of the mixtures by cooling occurs in the same mechanism of the 3-D Ising. In addition, the IR results reveal that the evolution of water clusters by hydrogen bonding progresses with the decrease in the temperature in the same way among the MCl−AN−water mixtures. According to both SANS and IR results, phase separation of the MCl−AN−water mixtures takes place as the hydrogen bonds among water molecules are three-dimensionally evolved around ions in the mixtures by cooling. However, the reason for the sequence of phase separation of the $Na^+ > K^+ > Li^+$ systems cannot be found in both results.

In contrast with the SANS and IR results, the ^7Li and ^{23}Na NMR relaxation rates for the MX−AN−water mixtures suggest the different solvation structure of Li^+ and Na^+ in the mixtures. Additionally, the relaxation rates reveal that the solvation structure of the alkali metal ions depends on the counteranions. The results of the ^7Li and ^{23}Na NMR chemical shifts agree with those of the relaxation rates. Both NMR results suggest that the hydration structure of Li^+ and Na^+ becomes more rigid with increasing x_{AN}. In particular, the hydration structure of Na^+ is strengthened even at $x_{AN} = 0.1$. This is consistent with the SANS results; thus, water clusters are more evolved in the Na^+ systems than the Li^+ ones at a given temperature. The ^7Li NMR relaxation rates and chemical shifts clearly show the solvation of acetonitrile molecules for Li^+ and the formation of $Li^+−Cl^-$ and $Li^+−Br^-$ contact ion pairs in the MX−AN−water mixtures. The evolution of water clusters in the mixtures may be significantly disturbed by the formation of contact ion pairs because the individual effects of cation and anion on water clusters are reduced. The two factors prevent the evolution of water clusters around Li^+, Cl^-, and Br^-. This is the main reasons for the higher phase-separation temperatures of the MX−AN−water mixtures in the sequence of NaX > KX > LiX (X = Cl^- and Br^-). In the sequence, the higher phase-separation temperature of the NaX systems than the KX can be readily understood by the magnitude of the hydration enthalpies of both cations. As the same, the lower phase-separation temperatures of the MBr systems compared with the MCl ones can be interpreted in terms of the hydration of anions. However, Li^+ ions strangely behave with acetonitrile, Cl^-, and Br^- in the LiX−AN−water mixtures. The limitation of the solubility of LiCl for the AN−water mixtures above $x_{AN} = 0.6$ also suggests the easy formation of $Li^+−Cl^-$ contact ion pairs. These are due mainly to the very high charge density of Li^+.

Since the beginning of this century, phase equilibria of solutions involving salts have often been revisited. Several researchers have succeeded in understanding their mechanism on the basis of Debye−Hückel[38] and Ginzburg−Landau[39,40] theories. Recently, the formation of ion pairs in aqueous solutions has been interpreted in terms of Hofmeister series[41] of the 19th century's idea; chaotropic cations may easily interact with chaotropic anions, whereas cosmotropic cations strongly interact with cosmotropic anions.[42] The present investigation experimentally gives the answer to the strange behavior of alkali halide series in the phase equilibria of AN−water mixtures, which is consistent with such previous investigations.

CONCLUSIONS

The present results showed that phase separation of the MX−AN−water mixtures (M = Li^+, Na^+, and K^+ and X = Cl^- and Br^-) occurs at higher temperature in the sequence of NaX > KX > LiX. This sequence differs from that of the magnitude of the hydration enthalpies ($Li^+ > Na^+ > K^+$). The SANS measurements revealed that water clusters in all of the three alkali chloride systems are evolved with the decrease in the temperature through the 3D-Ising mechanism. The IR results showed that the hydrogen bonds among water molecules are evolved in the MCl−AN−water mixtures in the same manner as the temperature decreases. Thus, both SANS and IR results did not clearly show the reason why phase separation of the LiX−AN−water mixtures less easily occurs compared with NaX− and KX−AN−water mixtures. In contrast, the ^7Li and ^{23}Na NMR experiments enabled us to clarify the different solvation structure between Li^+ and Na^+ in the LiX and NaX systems. The high charge density of Li^+ attracts not only water molecules but also acetonitrile ones. Thus, acetonitrile molecules may also solvate Li^+. Furthermore, the $Li^+−Cl^-$ and $Li^+−Br^-$ contact ion pairs may be formed in the LiX systems. NaCl does not significantly form ion pairs in the NaX systems. Thus, the two factors of the solvation of acetonitrile and the formation of ion pairs prevent the evolution of water clusters around Li^+, Cl^-, and Br^-. These are the reasons for the weaker effect of LiX on phase separation of the mixtures compared with the NaX and KX.

ASSOCIATED CONTENT

Supporting Information

Tables showing the ^7Li and ^{23}Na spin−lattice relaxation rates and chemical shifts of MX−AN−water mixtures at 298 K. Reference list with complete authors' names. This material is available free of charge via the Internet at http://pubs.acs.org.

AUTHOR INFORMATION

Corresponding Author

*E-mail: takamut@cc.saga-u.ac.jp.

Present Address

[†]Department of Chemical Biology and Applied Chemistry, College of Engineering, Nihon University, 1 Nakagawara, Tokusada, Tamura-machi, Koriyama, Fukushima 963−8642, Japan.

Notes

The authors declare no competing financial interest.

ACKNOWLEDGMENTS

This work was partially supported by Grant-in-Aid for Scientific Research (C) (no. 22550018) from the Japan Society for the Promotion of Science and Grant-in-Aid for Scientific Research on Innovative Areas "Earth Science Based on the High Pressure and Temperature Neutron Experiments" (no. 23103704) from the Ministry of Education, Culture, Sports and Technology, Japan. The SANS experiments were carried out under the Joint-use Research Program for Neutron Scattering, Institute for Solid State Physics (ISSP), the University of Tokyo, at the Research Reactor JRR-3, JAEA (proposal no. 10634). The density and NMR measurements for the sample solutions were conducted at the Analytical Research Center for Experimental Sciences of Saga University.

REFERENCES

(1) Schneider, G. Druckeinfluß auf die Entmischung flüssiger Systeme. *Z. Phys. Chem. (Muenchen, Ger.)* **1964**, *41*, 327−338.

(2) Ito, N.; Fujiyama, T.; Udagawa, Y. A Study of Local Structure Formation in Binary Solutions of 2-Butoxyethanol and Water by Rayleigh Scattering and Raman Spectra. *Bull. Chem. Soc. Jpn.* **1983**, *56*, 379−385.

(3) Armitage, D. A.; Blandamer, M. J.; Foster, M. J.; Hidden, N. J.; Morcom, K. W.; Symons, M. C. R.; Wootten, M. Thermodynamic, Ultrasonic, Spectroscopic and Miscibility Studies of Water + Methyl Cyanide Solutions. *J. Trans. Faraday Soc.* **1968**, *64*, 1193−1200.

(4) Roux, G.; Perron, G.; Desnoyers, J. E. Model Systems for Hydrophobic Interactions: Volumes and Heat Capacities of *n*-Alkoxyethanols in Water. *J. Solution Chem.* **1978**, *7*, 639−654.

(5) Moreau, C.; Douhéret, G. Thermodynamic Behavior of Water−Acetonitrile Mixtures Excess Volumes and Viscosities. *Thermochim. Acta* **1975**, *13*, 385−392.

(6) Easteal, A. J. Tracer Diffusion Coefficients of Tritiated Water and Acetonitrile in Water + Acetonitrile Mixtures. *Aust. J. Chem.* **1980**, *33*, 1667−1675.

(7) Ben-Naim, A. Inversion of the Kirkwood−Buff Theory of Solutions: Application to the Water−Ethanol System. *J. Chem. Phys.* **1977**, *67*, 4884−4890.

(8) Takamuku, T.; Tabata, M.; Yamaguchi, A.; Nishimoto, J.; Kumamoto, M.; Wakita, H.; Yamaguchi, T. Liquid Structure of Acetonitrile−Water Mixtures by X-ray Diffraction and Infrared Spectroscopy. *J. Phys. Chem. B* **1998**, *102*, 8880−8888.

(9) Nishikawa, K.; Kasahara, Y.; Ichioka, T. Inhomogeneity of Mixing in Acetonitrile Aqueous Solution Studied by Small-Angle X-ray Scattering. *J. Phys. Chem. B* **2002**, *106*, 693−700.

(10) Debye, P.; MacAulay, J. Das Elektrische Feld der Ionen und die Neutralsalzwirkung. *Phys. Z.* **1925**, *26*, 22−29.

(11) Long, F. A.; McDevit, W. F. Activity Coefficients of Nonelectrolyte Solutes in Aqueous Salt Solutions. *Chem. Rev.* **1952**, *51*, 119−169.

(12) Fromon, M.; Treiner, C. Scaled-Particle Theory and Salting Constant of Tetrahydrofuran in Various Aqueous Electrolyte Solutions at 298.15 K. *J. Chem. Soc., Faraday Trans. 1* **1979**, *75*, 1837−1848.

(13) Aveyard, R.; Heselden, R. Salting-out of Alkanols by Inorganic Electrolytes. *J. Chem. Soc., Faraday Trans. 1* **1975**, *71*, 312−321.

(14) Conway, B. E. Local Changes of Solubility Induced by Electrolytes: Salting-out and Ionic Hydration. *Pure Appl. Chem.* **1985**, *57*, 263−272.

(15) Haugen, G. R.; Friedman, H. L. Ion−Water Interaction ("Salting out") in Nitromethane and the Free Energy of Transfer of Some Electrolytes to Pure Nitromethane from Nitromethane Saturated with Water. *J. Phys. Chem.* **1963**, *67*, 1757−1761.

(16) Krishnan, C. V.; Friedman, H. L. Model Calculations for Setchenow Coefficients. *J. Solution Chem.* **1974**, *3*, 727−744.

(17) Hall, D. G. Kirkwood−Buff Theory of Solutions. An Alternative Derivation of Part of It and Some Applications. *Trans. Faraday Soc.* **1971**, *67*, 2516−2524.

(18) Takamuku, T.; Matsuo, D.; Yamaguchi, A.; Tabata, M.; Yoshida, K.; Yamaguchi, T.; Nagao, M.; Otomo, T.; Adachi, T. Small-Angle Neutron Scattering Study on Aggregation in Acetonitrile−D_2O and Acetonitrile−D_2O−NaCl Mixtures. *Chem. Lett.* **2000**, 878−879.

(19) Takamuku, T.; Yamaguchi, A.; Matsuo, D.; Tabata, M.; Kumamoto, M.; Nishimoto, J.; Yoshida, K.; Yamaguchi, T.; Nagao, M.; Otomo, T.; et al. Large-Angle X-ray Scattering and Small-Angle Neutron Scattering Study on Phase Separation of Acetonitrile−Water Mixtures by Addition of NaCl. *J. Phys. Chem. B* **2001**, *105*, 6236−6245.

(20) Takamuku, T.; Yamaguchi, A.; Matsuo, D.; Tabata, M.; Yamaguchi, T.; Otomo, T.; Adachi, T. NaCl-Induced Phase Separation of 1,4-Dioxane−Water Mixtures Studied by Large-Angle X-ray Scattering and Small-Angle Neutron Scattering Techniques. *J. Phys. Chem. B* **2001**, *105*, 10101−10110.

(21) Takamuku, T.; Nakamizo, A.; Tabata, M.; Yoshida, K.; Yamaguchi, T.; Otomo, T. Large-Angle X-ray Scattering, Small-Angle Neutron Scattering, and NMR Relaxation Studies on Mixing States of 1,4-Dioxane−Water, 1,3-Dioxane−Water, and Tetrahydrofuran−Water Mixtures. *J. Mol. Liq.* **2003**, *103/104*, 143−159.

(22) Gutmann, V. The Donor−Acceptor Approach to Molecular Interactions; Plenum Press: New York, 1978.

(23) Takamuku, T.; Noguchi, Y.; Yoshikawa, E.; Kawaguchi, T.; Matsugami, M.; Otomo, T. Alkali Chlorides-Induced Phase Separation of Acetonitrile−Water Mixtures Studied by Small-Angle Neutron Scattering. *J. Mol. Liq.* **2007**, *131/132*, 131−138.

(24) Marcus, Y. The Thermodynamics of Solvation of Ions. Part 2. The Enthalpy of Hydration at 298.15 K. *J. Chem. Soc., Faraday Trans.* **1987**, *83*, 339−349.

(25) Sadakane, K.; Onuki, A.; Nishida, K.; Koizumi, S.; Seto, H. Multilamellar Structures Induced by Hydrophilic and Hydrophobic Ions Added to a Binary Mixture of D_2O and 3-Methylpyridine. *Phys. Rev. Lett.* **2009**, *103*, 167803/1−167803/4.

(26) Okabe, S.; Nagao, M.; Karino, T.; Watanabe, S.; Adachi, T.; Shimizu, H.; Shibayama, M. Upgrade of the 32 m Small-Angle Neutron Scattering Instrument SANS-U. *J. Appl. Crystallogr.* **2005**, *38*, 1035−1037.

(27) Okabe, S.; Karino, T.; Nagao, M.; Watanabe, S.; Shibayama, M. Current Status of the 32 m Small-Angle Neutron Scattering Instrument, SANS-U. *Nucl. Instrum. Methods Phys. Res., Sect. A* **2007**, *572*, 853−858.

(28) Holz, M.; Sacco, A. Influence of the Debye−Hückel Ion−Ion Distribution on NMR Parameters of Ionic Nuclei. *Z. Phys. Chem. (Muenchen, Ger.)* **1987**, *155*, 133−143.

(29) Braun, B. M.; Holz, M. Separation of Local Asymmetry and Selective Solvation Effects Using the Quadrupole Relaxation of the $^{23}Na^+$ and $^{87}Rb^+$ Ions in Acetonitrile−Water Mixtures. *J. Solution Chem.* **1983**, *12*, 685−701.

(30) Mizuno, K.; Tamiya, Y.; Mekata, M. External Double Reference Method to Study Concentration and Temperature Dependences of Chemical Shifts Determined on a Unified Scale. *Pure Appl. Chem.* **2004**, *76*, 105−114.

(31) Momoki, K.; Fukazawa, Y. Bulbed Capillary External Referencing Method for Proton Nuclear Magnetic Resonance Spectroscopy. *Anal. Chem.* **1990**, *62*, 1665−1671.

(32) Momoki, K.; Fukazawa, Y. Bulbed Capillary External Referencing Method Using a Superconducting Magnet NMR Instrument. *Anal. Sci.* **1994**, *10*, 53−58.
(33) Takamuku, T.; Noguchi, Y.; Matsugami, M.; Iwase, H.; Otomo, T.; Nagao, M. Heterogeneity of Acetonitrile−Water Mixtures in the Temperature Range 279−307 K Studied by Small-Angle Neutron Scattering Technique. *J. Mol. Liq.* **2007**, *136*, 147−155.
(34) Stanley, H. E. *Introduction to Phase Transition and Critical Phenomena*; Oxford University Press: Oxford, U.K., 1971.
(35) Gebhardt, W.; Krey, U. *Phasenübergänge und Kritische Phänomene*, German edition; Vieweg: Braunschweig, Germany, 1980.
(36) Cupane, A.; Levantino, M.; Santangelo, M. G. Near-Infrared Spectra of Water Confined in Silica Hydrogels in the Temperature Interval 365−5 K. *J. Phys. Chem. B* **2002**, *106*, 11323−11328.
(37) Cartailler, T.; Kunz, W.; Turq, P.; Bellisent-Funel, M.-C. Lithium Bromide in Acetonitrile and Water: a Neutron Scattering Study. *J. Phys.: Condens. Matter* **1991**, *3*, 9511−9520.
(38) Moreira, A. G.; Netz, R. R. Phase Behavior of Three-Component Ionic Fluids. *Eur. Phys. J. D* **2001**, *13*, 61−66.
(39) Onuki, A.; Kitamura, H. Solvation Effects in Near-Critical Binary Mixtures. *J. Chem. Phys.* **2004**, *121*, 3143−3151.
(40) Onuki, A.; Okamoto, R.; Araki, T. Phase Transitions in Soft Matter Induced by Selective Solvation. *Bull. Chem. Soc. Jpn.* **2011**, *84*, 569−587.
(41) (a) Hofmeister, F. Zur Lehre von der Wirkung der Salze. *Arch. Exp. Pathol. Pharmakol.* **1888**, *24*, 247−260. (b) Kunz, W.; Henle, J.; Ninham, B. W. 'Zur Lehre von der Wirkung der Salze' (about the Science of the Effect of Salts): Franz Hofmeister's Historical Papers. *Curr. Opin. Colloid Interface Sci.* **2004**, *9*, 19−37.
(42) Vlachy, N.; Jagoda-Cwiklik, B.; Vácha, R.; Touraud, D.; Jungwirth, P.; Kunz, W. Hofmeister Series and Specific Interactions of Charged Headgroups with Aqueous Ions. *Adv. Colloid Interface Sci.* **2009**, *146*, 42−47.